Cardiac activation–repolarization patterns and ion channel expression mapping in intact isolated normal human hearts ⓔ

Tobias Opthof, PhD,[*†] Carol Ann Remme, MD, PhD,[*] Esther Jorge, DVM, PhD,[‡]
Francisco Noriega, MD,[‡] Rob F. Wiegerinck, PhD,[‡] Arlin Tasiam,[*] Leander Beekman,[*]
Jesus Alvarez-Garcia, MD,[‡] Cristian Munoz-Guijosa, MD, PhD,[§] Ruben Coronel, MD, PhD,[*¶]
Juan Cinca, MD, PhD[‡]

*From the [*]Department of Clinical and Experimental Cardiology, Heart Center Amsterdam, Amsterdam,
The Netherlands, [†]Department of Medical Physiology, University Medical Center Utrecht, Utrecht,
The Netherlands, [‡]Cardiology Service, Hospital de la Santa Creu i Sant Pau, IIb Sant Pau, Barcelona, Spain,
[§]Cardiac Surgery Service, Hospital de la Santa Creu i Sant Pau, IIb Sant Pau, Barcelona, Spain, and
[¶]IHU Institut de Rythmologie en Modélisation Cardiaque, Fondation Bordeaux Université, Bordeaux, France.*

BACKGROUND The repolarization pattern of the human heart is unknown.

OBJECTIVE The purpose of this study was to perform a multisite analysis of the activation–repolarization patterns and mRNA expression patterns of ion channel subunits in isolated human hearts.

METHODS Hearts from 3 donors without reported cardiac disease were Langendorff perfused with the patient's own blood. A standard ECG was obtained before explantation. Up to 92 unipolar electrograms from 24 transmural needles were obtained during right atrial pacing. Local activation and repolarization times and activation–recovery intervals (ARI) were measured. The mRNA levels of subunits of the channels carrying the transient outward current and slow and rapid components of the delayed rectifier current were determined by quantitative reverse transcriptase polymerase chain reaction at up to 63 sites.

RESULTS The repolarization gradients in the 3 hearts were different and occurred along all axes without midmural late repolarization. A negative activation–repolarization relationship

occurred along the epicardium, but this relationship was positive in the whole hearts. Coefficients of variation of mRNA levels (40%–80%) and of the Kv7.1 protein (alpha-subunit slow delayed rectifier channel) were larger than those of ARIs (7%–17%). The regional mRNA expression patterns were similar in the 3 hearts, unlike the ARI profiles. The expression level of individual mRNAs and of Kv7.1 did not correlate with local ARIs at the same sites.

CONCLUSION In the normal human heart, repolarization gradients encompass all axes, without late midmural repolarization. Last activated areas do not repolarize first as previously assumed. Gradients of mRNAs of single ion channel subunits and of ARIs do not correlate.

KEYWORDS Human heart; Repolarization pattern; Activation–recovery interval; Activation pattern; mRNA expression levels; Kv7.1 protein; Cardiac ion channel

(Heart Rhythm 2016;0:1–8) © 2016 The Authors. Published by Elsevier Inc. on behalf of Heart Rhythm Society. This is an open access article under the CC BY-NC-ND license (http://creativecommons.org/licenses/by-nc-nd/4.0/).

Introduction

The ventricular repolarization sequence determines the morphology of the T wave.[1] Dispersion of repolarization plays a major role in the genesis of ventricular arrhythmias.[2,3] Despite its clinical relevance, the repolarization

sequence of the human heart is essentially unknown. Only a few studies have explored the local repolarization times (RTs) in diseased hearts, and these recordings were limited to the endocardium or epicardium.[4–7] The local RT is the sum of the local activation time (AT) and the duration of the local action potential. The latter can be indirectly assessed by the duration of the activation-recovery intervals (ARIs) from local electrograms.[8]

Current cardiology textbooks sustain the assumption that the last areas to be activated repolarize first.[9] Therefore, a negative relationship between activation and RTs is presumed. However, Hanson et al[10] have shown that in patients undergoing cardiac surgery, the slope of the AT–RT

relationship is positive along the endocardium. In canine hearts, the AT–RT relationship also is positive.[11]

The intrinsic duration of the action potential is determined by the balance between inward and outward currents flowing during the plateau and repolarization phases. Thus, it can be anticipated that regional differences in expression of genes encoding for repolarizing channels will lead to different repolarization patterns.

This study was undertaken to assess the sequence and distribution of cardiac repolarization in relation to the activation process and local RNA expression of the ion channels carrying the major repolarizing currents in isolated perfused normal human hearts. The latter was quantitatively determined at the same locations where local electrograms were obtained, allowing direct correlation with ARI. The density of the alpha-subunit of the slow component of the delayed rectifier channel was measured as well. Our study does not permit a direct comparison between repolarization patterns and the T wave on the surface ECG.

Methods
Study material
We analyzed 3 human hearts obtained from organ donors with no reported cardiac disease but unsuitable for cardiac transplantation. These patients died because of irreversible cerebrovascular lesions at the Hospital de la Santa Creu i Sant Pau in Barcelona, Spain. Written informed consent for explantation had been obtained from the relatives. The hearts were extracted and immediately processed for experimental studies. The investigation conforms to the principles of the Declaration of Helsinki and was approved by the ethics review board of the hospital. Clinical variables, laboratory data, and conventional 12-lead ECG were obtained on admission and before cardiac explantation.

Electrical mapping and data analysis
The explanted hearts were Langendorff-perfused at 37°C and stimulated from the right atrium at cycle length of 700 ms. After an equilibration period of 30–60 minutes, local unipolar electrograms were simultaneously recorded (duration of each registration 2 seconds) from up to 24 transmural needles inserted in the left ventricle (LV) and septum (needles harboring 4 electrodes at 4-mm distance) and in the right ventricular (RV) (needles with 3 electrodes at 4-mm distance). In each electrogram, activation time (AT) and RTs were detected automatically as the moment of dV/dt_{min} during the QRS complex and the moment of dV/dt_{max} during the T wave (relative to the earliest start of the QRS complex in any of the electrodes),[8,12,13] respectively, as shown in Online Supplementary Figure 1. Subtraction of AT from RT yielded ARI. Activation, repolarization, and ARI patterns were manually constructed. To allow comparison with the molecular biologic data, ARI data were also expressed as a fraction of the average value of the entire heart (see Online Supplemental Material for details).

Molecular analysis
Myocardial samples were obtained from each heart adjacent to the sites with electrophysiologic data. Transmural samples were divided into equal epicardial, mid, and endocardial portions, except in the RV myocardium, which were divided into equal epicardial and endocardial portions. Each sample was immediately snap-frozen in liquid nitrogen and stored at –80°C. A maximum of 63 samples (18 RV, 18 septum, 27 LV) was obtained per heart.

mRNA transcript analysis
Quantitative polymerase chain reaction data of mRNAs encoding for alpha- and beta-units of the channels carrying I_{to}, I_{Ks}, and I_{Kr} were analyzed with the LinRegPCR program.[14] Samples were measured in duplicate and normalized to the housekeeping gene *HPRT*. Regional RNA expression is provided as a fraction relative to the average of the respective mRNA in the whole heart. Details of the isolation and sequences of primers are given in Online Supplementary Table 1.

Western blot analysis
For western blotting, 15 μg of total protein (whole cell lysate isolated from human heart tissue samples) was separated on a 4%–20% gradient SDS-PAGE gel and incubated with the following primary antibodies: anti-GAPDH (1:1000; catalog no. 10R-G109a, Fitzgerald Industries International, Acton, MA, USA) and anti-Kv7.1 (KCNQ1m 1:200; catalog no. APC-022, Alomone Labs, Jerusalem, Israel). All samples were blotted in triplicate, and results were represented as KCNQ1 density relative to glyceraldehyde-3-phosphate dehydrogenase (GAPDH). Details on protein isolation, blotting procedure, quantification, and data analysis are provided in the Online Supplemental Material.

Statistical analysis
Analysis of variance was used to test regional differences of local electrophysiologic variables. mRNA expression levels between regions of the heart were tested nonparametrically with the Kruskal–Wallis test. Post hoc analysis was performed by either the Student–Newman–Keuls test or by the Dunn test. AT–RT, mRNA-ARI, protein–ARI, and mRNA–protein relationships (all at the same sites) were analyzed using linear regression analysis. $P < .05$ was considered significant.

Results
Clinical findings
Table 1 summarizes the clinical, ECG, and echocardiographic data of the 3 donors. Online Supplementary Figure 2 shows normal T waves in donor 1 but negative T waves in donors 2 and 3 at the time of cardiac explantation. In the case of donor 2, the negative T waves are asymmetric and appear in leads V_4–V_6, whereas in donor 3 the negative T waves are symmetric and altered in all precordial leads. Donor 2 had a previous history of arterial hypertension, and the echocardiogram suggests mild-to-moderate LV hypertrophy.

Table 1   Clinical, ECG, and echocardiographic data

|	Donor 1	Donor 2	Donor 3
Gender	Female	Male	Male
Age (years)	73	66	68
Body mass index	26	21	30
Heart rhythm	Sinus	Sinus	Sinus
Heart rate (bpm)	72	62	76
PR Interval (ms)	198	160	110
QRS complex duration (ms)	78	85	80
QT interval (ms)	445	460	395
T-wave morphology	Normal	Negative asymmetric (V_4–V_6)	Negative symmetric (V_1–V_6)
T-wave Duration (ms)	280	175	160
T-wave peak to end (ms)	130	90	75
Left ventricular ejection fraction (%)	57	65	Not available
Left ventricular end-diastolic diameter (mm)	45	45	Not available
Septal thickness (mm)	11	15	Not available
Cause of death	Intraparenchymal cerebral hemorrhage	Ischemic stroke with intracranial hypertension	Intraparenchymal hemorrhage with intracranial hypertension
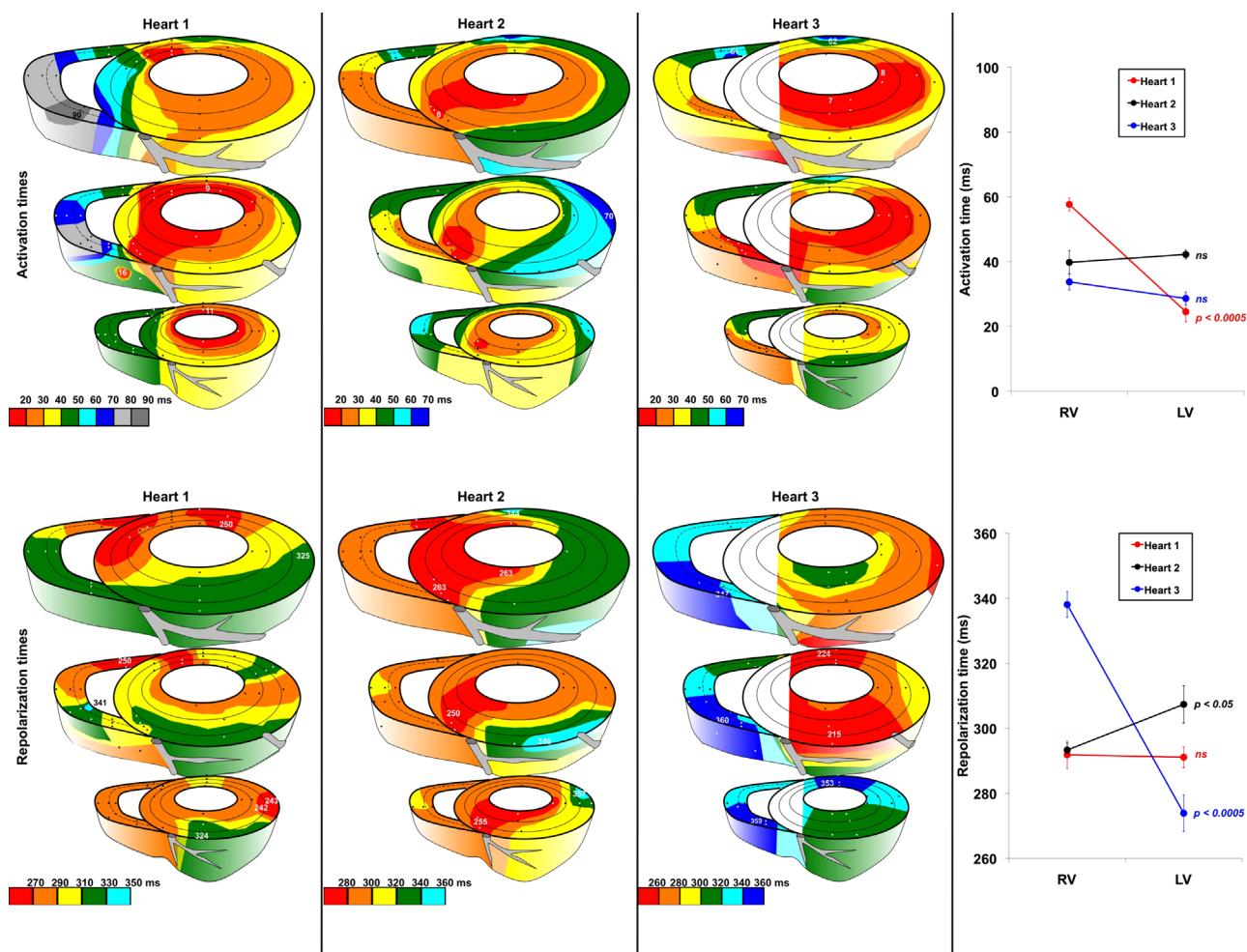
Figure 1   Activation patterns **(top panels)** and repolarization patterns **(bottom panels)** in the 3 studied isolated human hearts. Activation starts at the endocardium and follows an endocardial–epicardial sequence in the left ventricle (LV) and a sequence toward the base. Latest activation time was 90 ms in heart 1, 70 ms in heart 2, and 62 ms in heart 3. Repolarization gradients were 99 ms in heart 1, 108 ms in heart 2, and 145 ms in heart 3. **Right panels** summarize activation times and repolarization times in right ventricle (RV) and LV. Perfect signal-to-noise ratio permitted analysis of only 1 cardiac cycle for these patterns.

Electrophysiologic mapping

Figure 1 (top panels) shows that activation proceeds from the LV endocardium toward the LV epicardium in all hearts, corresponding to the report by Durrer et al.[15] The base of the hearts activates last. The total duration of local activation matches reasonably with the width of the QRS duration on the 12-lead ECG recorded before explantation in all cases. Differences in the pattern of repolarization among the 3 hearts are more pronounced (Figure 1, bottom panels). The total time from earliest to last repolarization (RT) is shorter in heart 1 (99 ms) than in heart 2 (108 ms) or in heart 3 (145 ms). The repolarization sequence in heart 1 starts at multiple sites (basal–posterior LV wall, central–posterior RV wall, and apical–lateral LV wall) and progresses toward the anterior region of the RV and LV. In heart 2, repolarization ends in the LV with a transmural gradient (epicardium repolarizing later than endocardium). In heart 3, repolarization ends in the right ventricle with—in addition—a prominent base-to-apex gradient in the LV. Figure 1 (right panels) shows that in heart 1 the absence of a left-to-right repolarization gradient is caused by compensation of the AT profile by the ARI profile. This is not the case in the 2 other hearts. Thus, the differences between the hearts are much larger during repolarization than during activation.

Figure 2 quantifies the dispersion in RTs of heart 1 along the major anatomic axes. The largest dispersion is found along the LV anterior–posterior axis. Figure 3 shows transmural gradients in RTs in detail in 12 needles with complete data in heart 1 (top panels, thin lines). In none of the needles is a midmural maximum in RT present. The bold lines show the averaged RTs (filled circles) and the averaged ARIs (open circles). In the LV, epicardial ARIs are shorter than endocardial ARIs, but not short enough to compensate for the duration of transmural activation. Figure 3 (bottom panel) shows the averaged transmural differences in RT in the LV for all data points in each heart, that is, including needles with missing data. Only in heart 2 are epicardial RTs

significantly later than endocardial RTs. In none of the hearts there is early epicardial repolarization or late midmural repolarization.

Table 2 provides the relationships between AT and RT in the 3 hearts. In the whole heart, the slope of this relationship is always positive (0.19, 1.15, and 0.15, respectively). In contrast, these relationships all are negative when only the epicardium is considered (–1.53, –1.92, and –0.14, respectively).

mRNA and protein expression

Online Supplementary Table 2 shows the expression levels of the 6 measured mRNAs encoding the alpha- and beta-subunits of the channels underlying the repolarizing currents I_{to} (KCND3 and KCNIP2), I_{Ks} (KCNQ1 and KCNE1), and I_{Kr} (KCNH2 and KCNE2) in all hearts. KCNIP2 has by far the highest expression level in all hearts, whereas KCNE2 has the lowest expression level. The differences in expression level between the hearts are significant for almost all mRNAs (see Online Supplementary Table 2 legend).

Figure 4 shows the distribution of mRNA values expressed as fraction of the average 1.0 for heart 1 together with its normalized ARIs. The left panels show regional variability in mRNA expression of the subunits associated with the channel carrying I_{to}. The alpha-subunit (KCND3)

Figure 3   Top panels: Transmural differences in repolarization time (RT) based on 12 needles with complete sets of data in the right ventricle (RV; n = 6) and left ventricle (LV; n = 6) in heart 1. Thin lines indicate individual RT values. Average RTs: filled circles (mean ± SEM.). Averaged ARIs: open circles (mean ± SEM). Bottom panel: Transmural repolarization times in the LV in the 3 hearts. All data points were included (also from needles with incomplete data). ARI = activation–recovery interval.
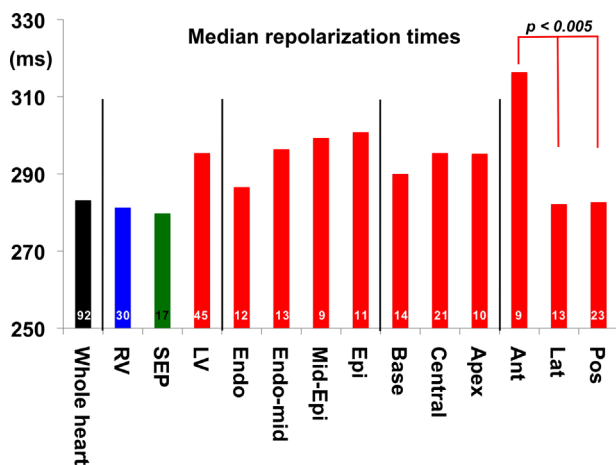

Figure 2   Median repolarization times in heart 1. Dissection over the parts (axes). LV = left ventricle; RV = right ventricle; SEP = septum. Further dissection of the LV data along the transmural axis [endocardium (Endo) to epicardium [Epi]], vertical axis (base to apex), and horizontal axis [anterior (Ant) to posterior (Pos)]. Number of sites indicated within the bars.
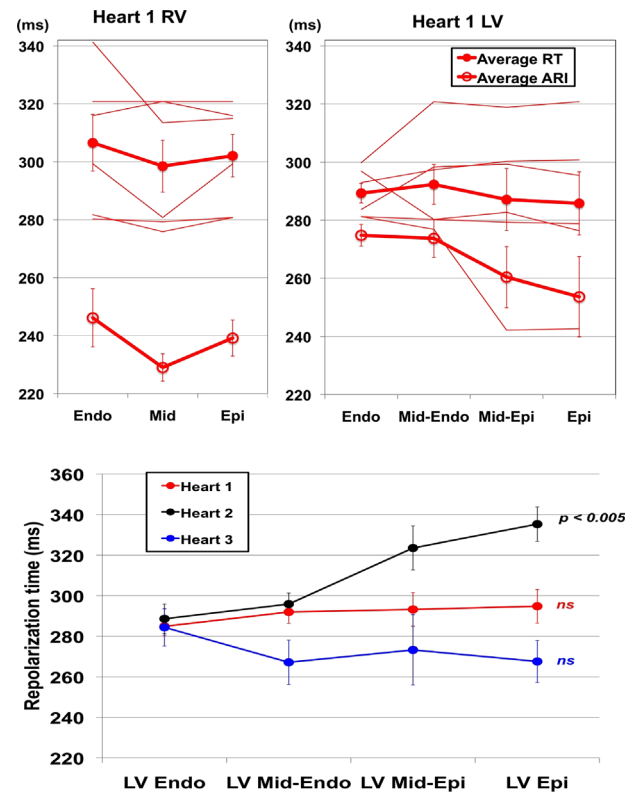
Table 2   Relationship between activation and activation–recovery intervals and between activation and repolarization in isolated human hearts

		Whole heart				Left ventricular epicardium			
		Function	n	r	P value	Function	n	r	P value
Heart 1	AT–ARI	y = −0.81x + 283	92	−0.611	.001	y = −2.53x + 349	11	−0.698	.05
	AT–RT	y = 0.19x + 283	92	0.183	NS	y = −1.53x + 349	11	−0.508	NS
Heart 2	AT–ARI	y = 0.15x + 252	52	0.119	NS	y = −2.92x + 451	6	−0.698	NS
	AT–RT	y = 1.15x + 252	52	0.680	.001	y = −1.92x + 451	6	−0.540	NS
Heart 3	AT–ARI	y = −0.85x + 294	71	−0.238	.05	y = −1.14x + 273	12	−0.392	NS
	AT–RT	y = 0.15x + 294	71	0.044	NS	y = −0.14x + 273	12	−0.053	NS

AT = activation time; ARI = activation–recovery interval; RT = repolarization time.

has higher expression in the LV than the RV. In contrast, the beta-subunit (*KCNIP2*) has a prominent transmural distribution pattern in the LV with higher subepicardial expression.

mRNA levels of the alpha-subunit of the channel carrying I_{Ks} (*KCNQ1*) are higher in the RV than in the LV (top panel, second column). The opposite is seen for the beta-subunit with prominent expression in the septum (*KCNE1*; bottom panel, second column).

In contrast to *KCNQ1*, the alpha-subunit of the channel carrying I_{Kr} (*KCNH2*) has higher mRNA expression levels in the LV than in the RV (top panel, third column), with little regional variability of the beta-subunit (*KCNE2*; bottom panel, third column).

The minimum and maximum ARIs are 200 ms (central–posterior RV) and 298 ms (basal–anterior LV). These values differ <25% from the average value of 252 ms. Thus, the
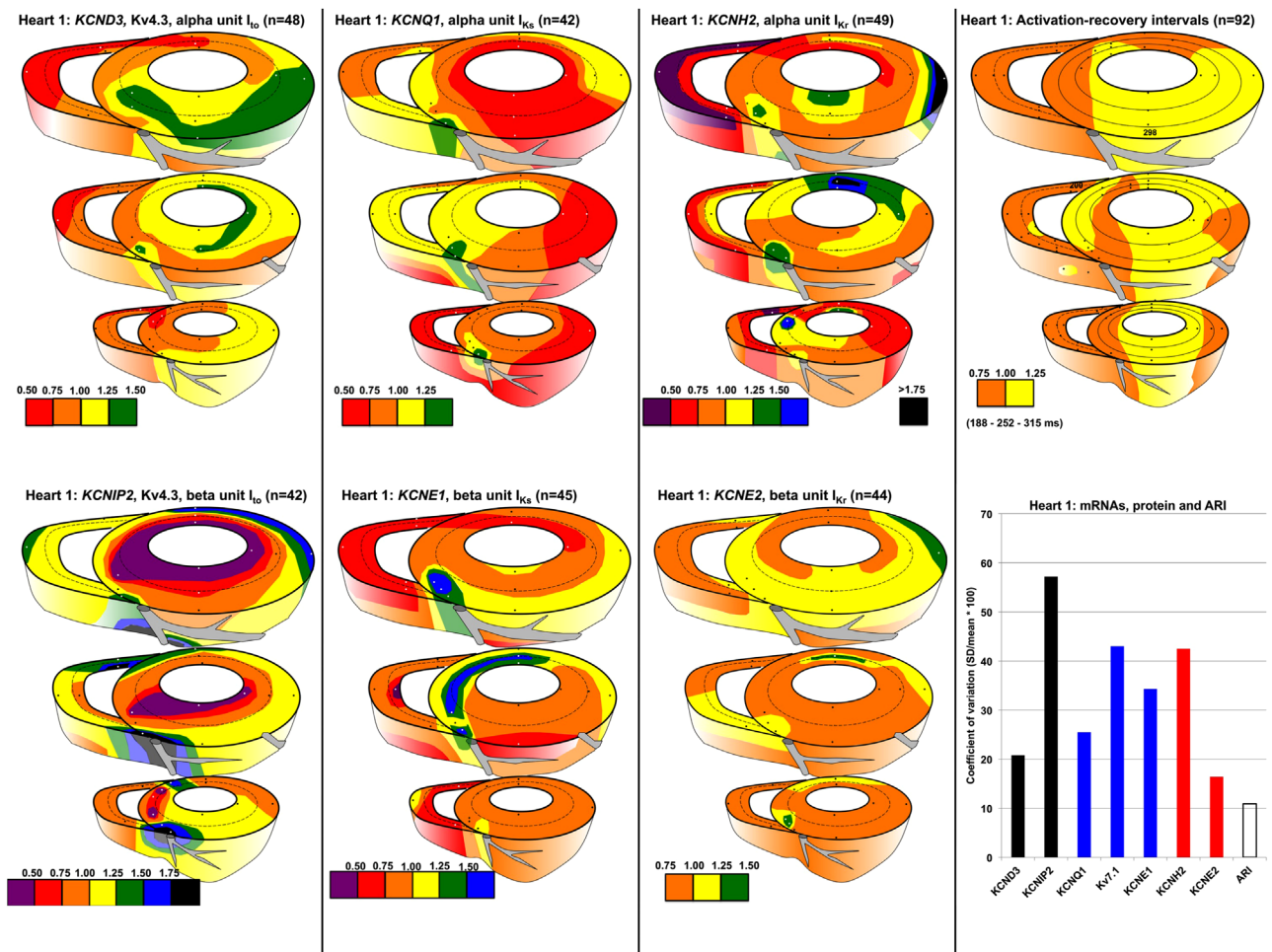

Figure 4   Regional relative expression levels of mRNAs and regional distribution activation–recovery intervals (ARIs) in heart 1. All values are relative to the mean of the whole heart (for real values see online Supplementary Table 2). **Left panels:** Subunits transient outward channel. **Mid-left panels** Subunits slow component of delayed rectifier channel. **Mid–right panels:** Subunits rapid component of delayed rectifier channel. **Right top panel:** ARIs. Shortest ARI = 200 ms; longest ARI = 298 ms. All ARIs expressed as fraction of averaged ARI (252 ms = 1.0). **Right bottom panel:** Coefficient of variation of the 6 mRNAs, 1 protein (Kv7.1; protein product of transcript *KCNQ1*) and of ARIs.

regional variability in dispersion of ARIs expressed as the coefficient of variation (SD/mean * 100) is (much) lower (11%) than that of any of the mRNAs (Figure 4, bottom right). Western blotting revealed that the regional variability of expression of Kv7.1, the protein resulting from translation of the transcript KCNQ1, is also substantially higher than that of ARIs. The same was observed in the other 2 hearts (see Online Supplementary Figure 3) with coefficients of variation for ARIs of only 7% and 17% in hearts 2 and 3, substantially lower than the regional dispersion in mRNAs and that of Kv7.1 in heart 3.

Because the RT patterns of the 3 hearts differed more than the AT patterns, we analyzed for each ion channel subunit the regional mRNA expression along the most relevant axes in greater detail. Overall, regional mRNA expression patterns (except for KCNQ1, see later) are similar in the 3 hearts. Figure 5 shows higher expression of KCND3 in the LV than in the RV in all hearts (top left panel). KCNIP2 shows inhomogeneity along the LV transmural axis (epi higher than endo; bottom left panel) but not along the RV–LV axis (data not shown).

There is no midmural minimum in KCNQ1 expression in any of the hearts (bottom second column). The expression profile of KCNQ1 along the RV–LV axis is the only one that differs between the hearts (top second column). KCNE1 has a remarkably similar regional distribution in all hearts, with highest expression in the septum (top third column), without a transmural difference. (bottom third column). In all hearts expression of KCNH2 is highest in the LV without midmural minimum (fourth column).

Absence of correlation between mRNA expression levels and ARIs

Figure 5 (right panels) shows that there are significant differences in ARIs along the LV–RV axis (top right panel) and that—in addition—these profiles differ between the hearts. These differences in ARIs are less apparent along the LV transmural axis (bottom right panel).

Online Supplementary Table 3 shows that none except 1 of 36 correlations between the expression level of the 6 transcripts and the ARIs recorded at the same sites in the RV and the LV of the 3 hearts is statistically significant. Although the expression profiles of KCND3, KCNE1, and KCNH2 are remarkably similar along the RV–LV axis (Figure 5) in the 3 hearts, the profile of KCNQ1 is different. Because this is also the case for the ARIs in the RV (Figure 5, top right panel), we focused on the relationship between KCNQ1 and ARIs in the RV in the 3 hearts in more detail. Online Supplementary Figure 4 shows that there is no significant correlation between local KCNQ1 expression and the ARIs, recorded at the same site, in the RV of individual hearts. However, the correlation across the 3 hearts is highly significant ($r = -0.726$, $P < .0005$, black dashed line in Online Supplementary Figure 4). Thus, it appeared as if variable KCNQ1 expression is relevant for ARI differences between hearts, but not within hearts. To better explore this concept, we performed western blots for Kv7.1 (the protein coded by KCNQ1) at selected sites in hearts 1 and 3. The selection focused on combinations of low and high KCNQ1 expression in combination with short and long ARIs, leading to 4 possible combinations. Heart 2 was excluded because not enough
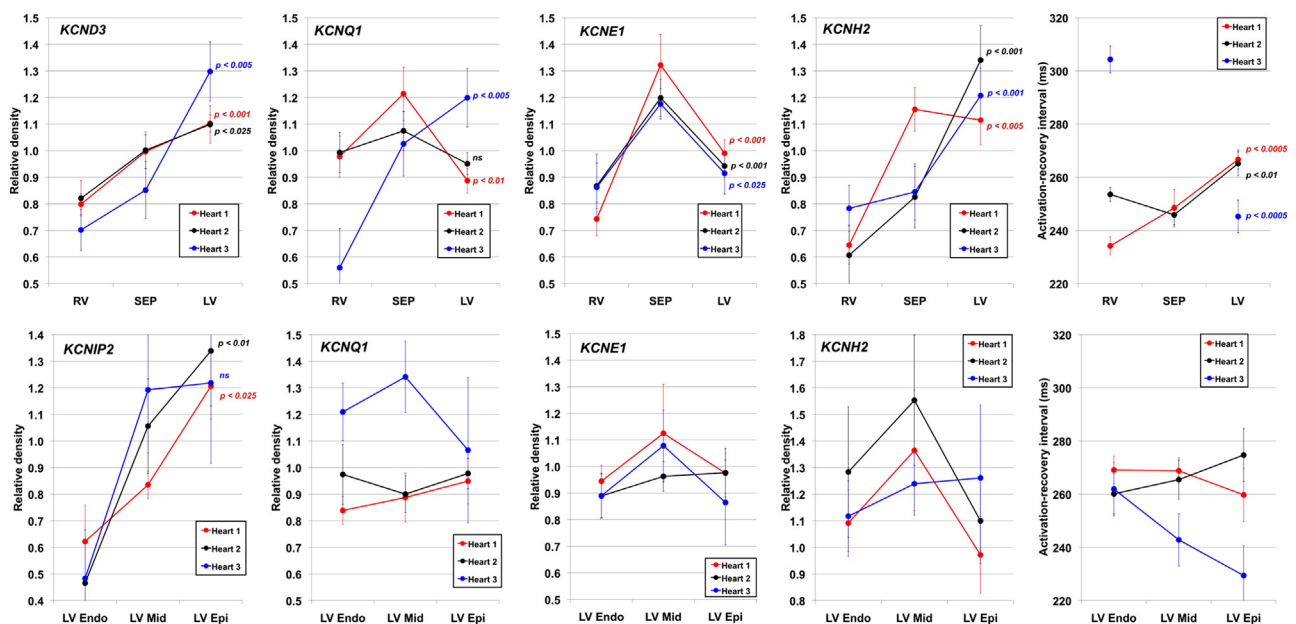

Figure 5   Regional expression levels of mRNAs and regional distribution activation–recovery intervals (ARIs) in the 3 hearts. Column 1: Alpha and beta subunits of transient outward channel. Column 2: Alpha subunit of the slow component of the delayed rectifier channel. Column 3: Beta subunit of the slow component of the delayed rectifier channel. Column 4: Alpha subunit of the rapid component of the delayed rectifier channel. **Right panels:** Distribution of ARIs. **Top panels:** Right ventricle (RV), left ventricle (LV), and septum (SEP) axis. **Bottom panels:** LV transmural axis. KCNQ1 is presented along both anatomic axes. Online Supplementary Table 2 provides the real mRNA values, the mean of which are set to 1.0 for each mRNA in each heart.
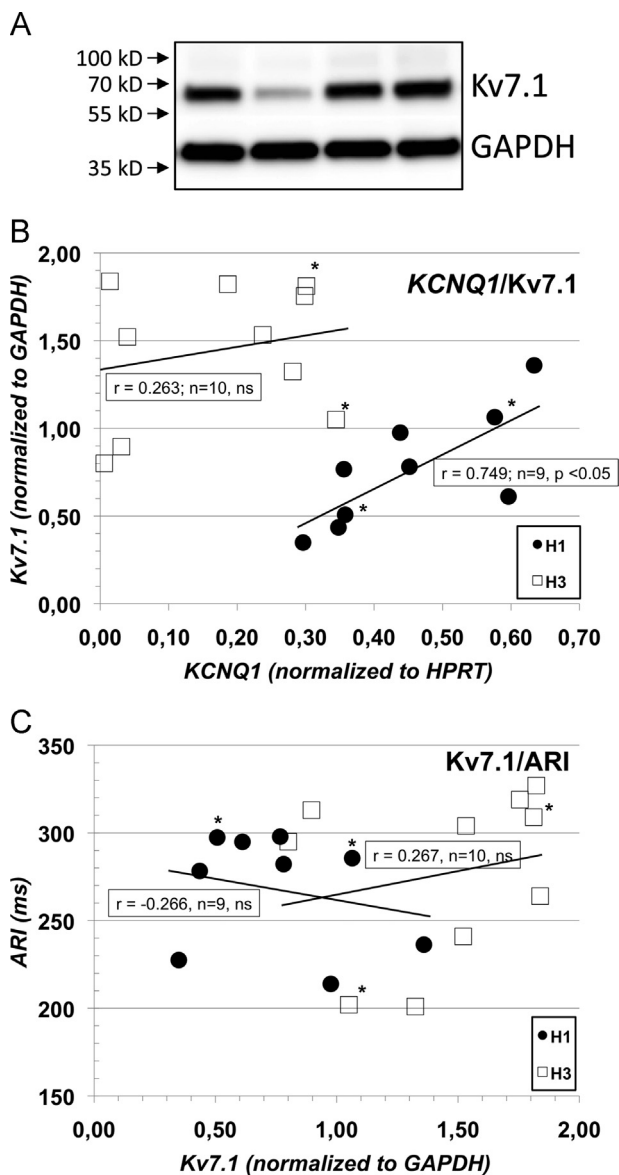
Figure 6 **A:** Representative western blots of KCNQ1/Kv7.1 and glyceraldehyde-3-phosphate dehydrogenase (GAPDH) (loading control) from 4 different sites in heart 1 (molecular weight markers indicated). **B:** Correlation of *KCNQ1* transcript of *KCNQ1* vs KCNQ1 protein (Kv7.1 density corrected for GAPDH) levels in hearts 1 and 3 (H1, H3). *Asterisks* indicate midmural sites. **C:** KCNQ1 protein levels (Kv7.1 density corrected for GAPDH) vs activation–recovery intervals (ARIs) in hearts 1 and 3 (H1, H3). *Asterisks* indicate midmural sites.

tissue was available. Figure 6A shows the density of the Kv7.1 protein at 4 sites from heart 1. Figure 6B shows a moderately positive (and significant) correlation between *KCNQ1* and Kv7.1 in heart 1 but not in heart 3. Figure 6C shows the absence of a relationship between the density of Kv7.1 and the ARIs within the hearts, compatible with our observations on mRNA and ARIs (see Online Supplementary Table 3). There were no midmural sites (indicated with an asterisk in Figures 6B and 6C) with lowest protein expression levels.

Discussion
Main findings
This study is the first analysis of the repolarization pattern of isolated perfused intact human hearts from donors free of significant cardiac disease, which includes transmural data. We found that in contrast to the well-defined endocardial to epicardial activation sequence in the LV, the repolarization pattern does not follow a specific pattern, starting at multiple sites and creating gradients along various cardiac axes although without midmural peak values. These repolarization patterns varied more between the hearts than the activation patterns, but this variability should be regarded with extreme caution, given the small number of hearts in this study. Correlations between activation and repolarization were weak, but they were positive when the whole heart was taken into account and negative when only the epicardium was considered. This last observation is in line with previous reports of the human heart[4–6] and is the prevailing explanation for concordance of polarity of QRS complex and T wave in textbooks.[9] Concurrent mapping of mRNA expression levels of alpha- and beta-subunits of the ion channels carrying I_{to}, I_{Kr}, and I_{Ks} showed large agreement between the hearts but virtually no relationship with local ARIs. The same was observed for the Kv7.1 protein, the alpha-subunit of the I_{Ks} channel.

Activation and repolarization gradients
Although the total AT of the hearts matched the duration of the QRS complex on the donor's 12-lead ECG, the period between earliest and latest repolarization was much shorter than the duration of the T wave. This repolarization mismatch corresponds to what was analyzed recently in the pig[1] and is explained because the cellular repolarization process starts much earlier than the moment of local repolarization (RT). RT as used in this study closely corresponds with the time of APD_{80}, when the myocytes are almost completely repolarized.[13] Our study does not permit a comparison between the repolarization pattern and the T wave on the patient's ECG because they were not simultaneously acquired.

Recently, a study in isolated perfused porcine heart with simultaneous recording of local electrograms and pseudo-ECG signals from electrodes distributed along a bucket filled with perfusion fluid revealed that the morphology of the T wave of the ECG was mainly determined by repolarization gradients in the entire heart and not along a single particular anatomic axis.[1] In accordance with that study, our study of 3 human hearts with different T-wave polarities also showed repolarization gradients along the whole heart, but not along the transmural axis in particular. The duration of the total repolarization gradient in the heart with positive T waves (heart 1, 99 ms) was shorter than that recorded in the other 2 hearts with negative T waves. The T wave of these 2 patients may have evolved to a negative pattern in concurrence with the development of intracranial hypertension, thus suggesting a neurogenic related mechanism.[16]

Relation to molecular data in man

mRNA expression levels of membrane channel subunits relevant for action potential duration have been reported previously in normal donor hearts, but not with a regional resolution as in our study.[17–19] Therefore, we were able to demonstrate regional differences within a heart that are of the same order of magnitude, or larger, than those between hearts (Figure 4 and Online Supplementary Table 2). Thus, single sample analyses in other studies should be interpreted with caution, especially if the site of origin is not the same among hearts.

The relationship between transcript and protein expression in general is not straightforward because of posttranscriptional regulation (see Chick et al[20] for references). We show a weak but moderately positive correlation between the *KCNQ1* transcript and its Kv7.1 protein in 1 heart but not in the other (Figure 6B). Gaborit et al[17] reported "good agreement" between transcript and protein expression for *KCND3* and *KCNIP2* without actually quantifying this relation. We could not confirm the strict linear and highly significant relationship between transcript, protein, and I_{to} as for the beta-unit of the I_{to} channel in the dog,[21] for transcript and protein of the alpha-subunit of the slowly activating delayed rectifier channel, and ARIs in the human heart. The reason that we could not confirm this strict relationship between mRNA, protein, and function (see Online Supplementary Table 3, and Figures 6B and 6C), may be as follows. (1) We measured in whole hearts (electrotonus) and not in single myocytes. (2) We measured ARIs, which result from a composite of many membrane currents. (3) The regional variability in *KCNIP2* is much higher than for the other transcripts (as is its expression level). (4) We measured in man and not in dog.

We speculate that the lower coefficient of variation in ARIs than in expression of any of the mRNAs reflects that cardiomyocytes are electrotonically coupled and therefore regional electrophysiologic differences are moderated, whereas mRNA and protein expression are not.

Repolarization of the human heart progresses along various anatomic axes and is not correlated to mRNA expression of single ion channels and also not to the protein expression of one of them.

Acknowledgment

Appendix
Supplementary data

Supplementary data associated with this article can be found in the online version at http://dx.doi.org/10.1016/j.hrthm.2016.10.010.

References

1. Meijborg VMF, Conrath CE, Opthof T, Belterman CNW, De Bakker JMT, Coronel R. The electrocardiographic T-wave and its relation with ventricular repolarization along major anatomical axes. Circ Arrhythmia Electrophysiol 2014;7:524–531.
2. Han J, Moe GK. Nonuniform recovery of excitability in ventricular muscle. Circ Res 1964;14:44–60.
3. Coronel R, Wilms-Schopman FJG, Opthof T, Janse MJ. Dispersion of repolarization and arrhythmogenesis. Heart Rhythm 2009;6:537–543.
4. Franz MR, Bargheer K, Rafflenbeul W, Haverich A, Lichtlen PR. Monophasic action potential mapping in human subjects with normal electrocardiograms: direct evidence for the genesis of the T wave. Circulation 1987;75:379–386.
5. Cowan JC, Hilton CJ, Griffiths CJ, Tansuphaswadikul S, Bourke JP, Murray A, Campbell RW. Sequence of epicardial repolarisation and configuration of the T wave. Br Heart J 1988;60:424–433.
6. Yuan S, Kongstad O, Hertervig E, Holm M, Grins E, Olsson B. Global repolarization sequence of the ventricular endocardium: monophasic action potential mapping in swine and humans. Pacing Clin Electrophysiol 2001;24:1479–1488.
7. Chauhan VS, Downar E, Nanthakumar K, Parker JD, Ross HJ, Chan W, Picton P. Increased ventricular repolarization heterogeneity in patients with ventricular arrhythmia vulnerability and cardiomyopathy: a human in vivo study. Am J Physiol Heart Circ Physiol 2006;290:H79–H86.
8. Haws CW, Lux RL. Correlation between in vivo transmembrane action potentials durations and activation-recovery intervals from electrograms. Effects of interventions that alter repolarization time. Circulation 1990;81:281–288.
9. Mirvis DM, Goldberger AL. Electrocardiography. In: Zipes DP, Libby P, Bonow RO, Braunwald E, eds. Braunwald's Heart Disease, Seventh Edition. Philadelphia, PA: Elsevier Saunders; 2007:107–151.
10. Hanson B, Sutton P, Elameri N, Gary M, Critchley H, Gill JS, Taggart P. Interaction of activation-repolarization coupling and restitution properties in humans. Circ Arrhythmia Electrophysiol 2009;2:162–170.
11. Opthof T, Coronel R, Janse MJ. Is there a significant transmural gradient in repolarization time in the intact heart? Repolarization Gradients in the Intact Heart. Circ Arrhythmia Electrophysiol 2009;2:89–96.
12. Coronel R, De Bakker JMT, Wilms-Schopman FJ, Opthof T, Linnenbank AC, Belterman CN, Janse MJ. Monophasic action potentials and activation-recovery-intervals as measures of ventricular action potential duration. Experimental evidence to resolve some controversies. Heart Rhythm 2006;3:1043–1050.
13. Potse M, Vinet A, Opthof T, Coronel R. T-wave polarity and measures of repolarization in unipolar electrograms in the isolated whole-heart preparation. Am J Physiol Heart Circ 2009;297:H792–H801.
14. Ruijter JM, Ramakers C, Hoogaars WMH, Karlen Y, Bakker O, van den Hoff MJB, Moorman AFM. Amplification efficiency: linking baseline and bias in the analysis of quantitative PCR data. Nucleic Acids Res 2009;37:e45.
15. Durrer D, Van Dam RT, Freud GE, Janse MJ, Meijler FL, Arzbaecher RC. Total excitation of the isolated human heart. Circulation 1970;41:899–912.
16. Burch GE, Meyers R, Abildskov JA. A new electrocardiographic pattern observed in cerebrovascular accidents. Circulation 1954;9:719–723.
17. Gaborit N, Varro A, Le Bouter S, Szuts V, Escande D, Nattel S, Demolombe S. Gender-related differences in ion-channel and transporter subunit expression in non-diseased human hearts. J Mol Cell Cardiol 2010;49:639–646.
18. Gaborit N, Le Bouter S, Szuts V, Varro A, Escande D, Nattel S, Demolombe S. Regional and tissue specific transcript signatures of ion channel genes in the non-diseased human heart. J Physiol 2007;582:675–693.
19. Ambrosi CM, Yamada KA, Nerbonne JM, Efimov IR. Gender differences in electrophysiological gene expression in failing and non-failing human hearts. PLoS ONE 2013;8:e54635.
20. Chick JM, Munger SC, Simecek P, Huttlin EL, Choi K, Gatti DM, Raghupathy N, Svensson KL, Churchill GA, Gygi SP. Defining the consequences of genetic variation on proteome-wide scale. Nature 2016;534:500–505.
21. Rosati B, Grau F, Rodriguez S, Li H, Nerbonne JM. Concordant expression of KChIP2 mRNA, protein and transient outward current throughout the canine ventricle. J Physiol 2003;548:815–822.